

Metastable states in undoped and doped a -Si:H studied by photomodulation spectroscopy

L. Chen and J. Tauc

*Division of Engineering, Brown University, Providence, Rhode Island 02912
and Department of Physics, Brown University, Providence, Rhode Island 02912*

J. Kočka and J. Stuchlík

*Institute of Physics of the Czechoslovak Academy of Sciences, Cukrovarnická 10, 162 00 Prague 6, Czechoslovakia
(Received 27 December 1991; revised manuscript received 30 March 1992)*

Changes in the gap states in undoped, phosphorus-, and boron-doped a -Si:H produced by light soaking (LS), thermal quenching (Q), and annealing (A) are studied by photomodulation spectroscopy. First a method for analyzing the photomodulation spectra is explained and applied to annealed samples. Then the changes in the spectra produced by LS and Q are analyzed. It is shown that LS increases the density of dangling bonds D_i in undoped a -Si:H. In a -Si:H:P, LS increases the density of dangling bonds D_p relative to the density of P_4 states. The LS a -Si:H:P samples also exhibit, in addition to D_p defects, defects with similar properties as D_i defects in undoped a -Si:H. This is a strong support for the presence of more than one kind of defect in a -Si:H:P. In a deposited boron-doped a -Si:H a region of photoinduced transmission was observed that disappears with A, LS, or Q. This change is irreversible, and the spectra of A, LS, or Q samples differ very little. The results are compared with the recent work on metastable states based on different methods.

I. INTRODUCTION

It is well established that the electric and photoelectric properties of undoped and doped a -Si:H can be changed by thermal treatment or light soaking. These effects are interpreted as evidence of the metastability of the states in the gap. Changes in conductivity and photoconductivity of undoped and doped a -Si:H produced by light soaking (LS) were observed by Staebler and Wronski.¹ Due to its practical importance, this metastability has been extensively studied and attributed to the deep defect generation, mediated by hydrogen motion.¹⁻⁶ Moreover, light soaking allows easy reversible change of the density of defects. The understanding of the nature and energy levels of deep defects(s) is of basic scientific and technological importance.

Street *et al.*⁷ found that rapid thermal quenching (Q) of doped a -Si:H from temperatures close to the deposition temperature increases the density of the tail states relative to the deep defects;^{3,6} this effect is also reversible by annealing (A). The LS and Q effects change the relative density of deep vs shallow states in opposite directions.

Many of the experimental results have been successfully explained by a model proposed by Street, Zsch, and Thomson.⁸ In this model, the only deep defect is the silicon dangling bond with a positive correlation energy. It has three different charge states (D^0 , D^+ , and D^-) with different energy levels, which can be converted one into another by changing the position of the Fermi level by doping or illumination. There are, however, some experimental results^{9,10} that cannot be explained by this model. That is the reason why the intimate pair model^{9,10} for doped a -Si:H or, later, a more general defect pool model¹¹

have been introduced. Their common feature is that there is more than one defect.

In undoped a -Si:H, the main defect has been associated with the dangling bond; we will refer to it as the intrinsic defect D_i . This defect is neutral in the dark (D_i^0), and traps an electron or a hole upon illumination (D_i^- or D_i^+). In phosphorus-doped samples (a -Si:H:P) the main deep defect is associated with phosphorus doping and we refer to it as D_p . This defect is in the D_p^- state in the dark, and becomes neutral D_p^0 after trapping a photogenerated hole. Similarly, in boron-doped a -Si:H (a -Si:H:B), the defect in the dark is D_B^+ which becomes neutral (D_B^0) after trapping a photogenerated electron; the energies of D_B^+ and D_B^0 are the same (by definition) if the lattice relaxation is negligible.

The photomodulation (PM) spectroscopy is a unique and sensitive tool for the study of the energy levels of defects that can exist in different charged states.¹² Changes in the photomodulation spectra of a -Si:H:P produced by LS were observed by Zhou¹³ as a shift of the peak of the PM spectrum toward higher energy upon LS; however, no detailed study has been done. A systematic study of the effect of LS, Q, and A processes on the PM spectra of a -Si:H, a -Si:H:P, and a -Si:H:B is the subject of this paper, with the aim of determining the changes in the gap states produced by these treatments.

II. EXPERIMENT

For this work, we used a steady-state photomodulation setup with an Ar⁺ laser as the pump (photon energy 2.4 eV, intensity 100 mW/cm²). The probe photon energy was in the range 0.06–2 eV. In the range 0.06–0.30 eV, we used a Fourier-transform infrared spectrophotometer

(Bomen model DA-3.01); the PM spectra were determined as the difference of the spectra measured with the pump on and off. In the range of 0.25–2 eV, we used a grating monochromator; the pump was chopped at 75 Hz. We measured photoinduced changes in transmission ΔT . The system's spectral response function was canceled by taking the ratio $\Delta T/T$. It has been shown that¹⁴ in *a*-Si:H, the relative changes in reflectivity $\Delta R/R$ in our spectral range are small compared to $\Delta T/T$. In this case, $-\Delta T/T$ is equal to the relative change in the absorption coefficient $\Delta\alpha/\alpha_p$ (provided the sample thickness d is larger than the pump absorption length α_p^{-1}). The spectral resolution was better than 50 (grating monochromator) and 5 meV (Fourier-transform spectrometer). The value of $-\Delta T/T$ was in the range 10^{-5} – 10^{-3} .

The samples were prepared by glow discharge (at 13 MHz) decomposition of pure saline (Si:H_4) to which the doping gases (PH_3 or B_2H_6) were added. The PH_3 -to- SiH_4 ratio was 10^{-4} , 10^{-3} , and 10^{-2} ; the B_2H_6 -to- SiH_4 ratio was 10^{-3} . The substrates (sapphire and single-crystal Si) were heated to 250 °C, the optimum temperature for the preparation of high-quality *a*-Si:H. The typical values of flow rate of SiH_4 and pressure are 30 scm and 0.2 mbar. Thick boron-doped samples had a tendency to peel off more easily than other samples.

LS was produced by a pulsed Nd:YAG (yttrium-aluminum-garnet) laser. Photon energy was 2.34 eV, pulse duration was 10 nsec, the pulse intensity was 2×10^4 W/cm², and the repetition rate was 20 Hz (the average power was 4 mW/cm²). The exposure time varied from 1 to 4 h. This LS is heavier than in most experiments in which LS is produced by a continuous exposure. Stutzmann, Biegelsen, and Tsai^{15,16} have shown that the density of defect states generated by LS in *a*-Si:H is proportional to $I^{3/2}t_{il}^{1/3}$, where I is the intensity of the LS beam and t_{il} is the time of exposure. It follows that increasing the power is much more efficient than increasing the time of exposure. A continuous exposure intensity equivalent to our pulsed exposure would be about 10 W/cm². This is to be compared with the pump average intensity of the order of 100 mW/cm² used in cw LS. During the measurements (which lasted up to 45 min) we did not observe light-induced changes in the samples.

For the thermal treatments, the sample was placed in a furnace at 200 °C for 2 h in the air, and then either slowly cooled (cooling rate was about 0.2 K/sec) (annealing A) or the substrate was rapidly cooled by flowing cold water (cooling rate was about 50 K/sec) (thermal quenching Q).

III. PM SPECTRUM OF ANNEALED SAMPLES

Before we deal with the changes in the PM spectra produced by LS and Q we will discuss the PM spectra of annealed samples which are shown in Figs. 1(a)–1(c). We measured these spectra on our samples and found that they are similar to those reported previously by Vardeny *et al.*¹⁷ We use here the model proposed in Ref. 17, which we partly modify and further develop.

The PM spectrum of undoped *a*-Si:H measured at 240

K [Fig. 1(a)] is ascribed to a superposition of pump-induced transitions producing increased absorption (PA) and transitions eliminated by the pump producing bleaching (PB). These transitions are schematically shown in the inset in Fig. 1(a). Absorption in the dark is due to transitions from the neutral dangling-bond state D_i^0 into the conduction band (CB), and also the transitions from the valence band (VB) into D_i^0 ; because of the positive electron correlation energy, the final state D_i^- is at a higher energy than D_i^0 . Therefore, we refer to this transition as $\text{VB} \rightarrow D_i^-$. These transitions are eliminated

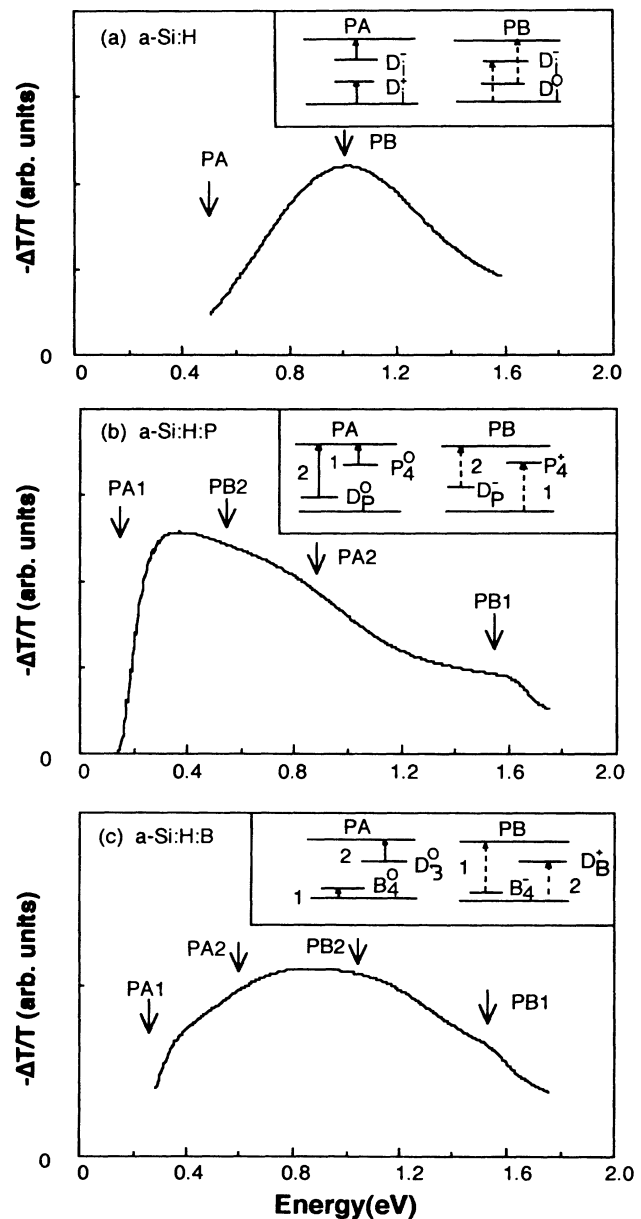


FIG. 1. PM spectra of annealed samples. The energy levels used for interpreting the spectra are shown in the insets. The transitions are indicated both in the insets and on the spectra, as explained in the text.

(PB) when the carriers generated by the pump change the D_i^0 defect to D_i^- or D_i^+ (by definition, D_i^+ in the absence of lattice relaxation has the same energy as D_i^0). These charged states generate new transitions $VB \rightarrow D_i^+$ and $D_i^- \rightarrow CB$, which produce increased absorption (PA). Since only one PM band is observed, one assumes that all transitions are symmetrical about the midgap.¹⁷ The defect states have a distribution about the peak energy which we refer to as the “defect energy”; because of the distributions, the onset energies differ from the defect energies.¹⁸

The PM spectra of a -Si:H:P [Fig. 1(b)] involve the dangling-bond D_p (which is in the D_p^- state in the dark) but also the band-tail (BT) states¹⁹ which contain the impurity P_4 states; we label them jointly as P_4 . The onset of the PM spectrum is transition $P_4^0 \rightarrow CB$ (PA1), followed by a decrease of absorption due to the bleaching of the $D_p^- \rightarrow CB$ transition (PB2). The high-energy PM band is produced²⁰ by the $D_p^0 \rightarrow CB$ (PA2) transition followed by the bleaching of the $VB \rightarrow P_4^+$ transition (PB1).

The onset of the PM spectra of a -Si:H:B [Fig. 1(c)] is the $VB \rightarrow B_4^0$ transition (PA1) followed by the $D_B^0 \rightarrow CB$ transition (PA2). There are two PB transitions, the $VB \rightarrow D_B^+$ transition (PB2) followed by the $B_4^- \rightarrow CB$ (PB1) transition (PB2 was not resolved in the data of Ref. 17). The spectrum of a -Si:H:B has broad features and therefore its analysis gives much less information than the analysis of the PM spectra of a -Si:H and a -Si:H:P.

For a more detailed analysis of the PM spectra, we have to take into account that the electronic states shown schematically in Fig. 1 have distributions. The distributions of the dangling bonds were assumed to be Gaussian. For the “intrinsic” D -states (in a -Si:H),

$$g_i(E) = A_i \exp[-(E - E_i)^2 / (\Delta E_D)^2]. \quad (1)$$

For the P- and B-doped samples, the density of states (DOS) is $g_P(E)$ and $g_B(E)$, given by Eq. (1) but replacing i by P or B, respectively. The DOS distributions of the neutral and the corresponding charged state were assumed to be the same.

The band-tail (BT) state distributions are assumed to be exponential.²¹ We write, for the CB tail,

$$g_T^c(E) = B_c \exp[-(E_c - E)/E_0^c]. \quad (2)$$

The equation is the same for the VB BT (replacing index c by v).

The PM spectrum is produced by the electron redistribution over the gap states generated by the pump. In the dark, the Fermi distribution a -Si:H has the Fermi energy E_F in the middle of the gap; in a a -Si:H:P (a -Si:H:B), E_F is in the CB (VB) band tail. Under illumination, the electron distribution is determined by the statistics developed by Simmons and Taylor;²² one has to take into account the correlation energies of the dangling bonds as discussed by Adler and Yoffa.²³ The characteristic parameters are the quasi-Fermi levels of electrons (F_n) and holes (F_p) defined in Ref. 22. In annealed samples, in the range of illumination levels used in this work, there is no dependence of the shape of the PM spectra associated with defects on the illumination level. This means that the

quasi-Fermi levels (which depend on the illumination level) F_n and F_p are outside the defect state distributions. Illumination changes the charge state of the dangling bond. For example, in a -Si:H, all D_i^0 states are transformed into D_i^- and D_i^+ states (illumination is strong enough to produce saturation of the defect states).

In doped samples, we must consider the changes in the occupation of the BT states. In the P-doped sample, the

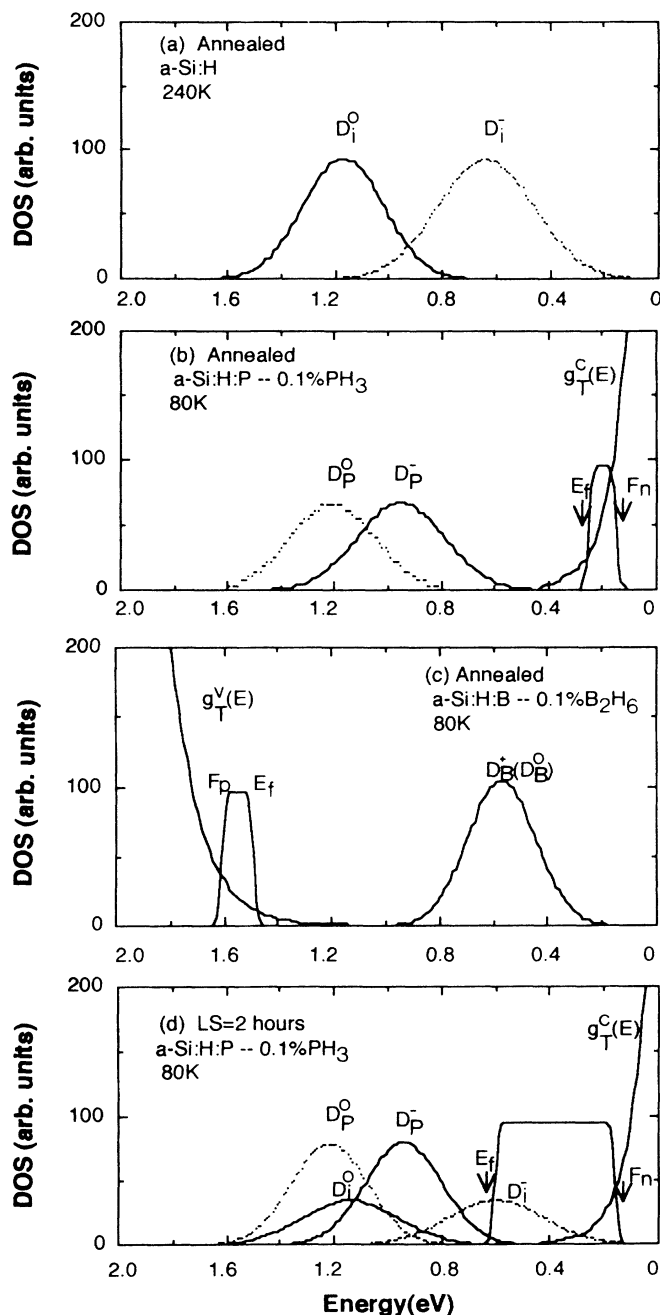


FIG. 2. Density of states in the gap as determined from the PM spectra of annealed undoped and doped a -Si:H [(a), (b), and (c)] and LS a -Si:H:P [(d)]. The relative intensities of the various bands are arbitrary.

DOS distribution of this change is

$$\Delta n_c(E) = g_c(E)[f(E, F_n) - f(E, E_f)], \quad (3a)$$

where

$$f(E, E_f) = \{\exp[(E - E_f)/kT] + 1\}^{-1}, \quad (3b)$$

$$f(E, F_n) = \{\exp[(E - F_n)/kT] + 1\}^{-1} \quad (3c)$$

(and similarly for the VB tail in boron-doped samples). Equation (3c) is only an approximation,²² valid in doped (extrinsic) samples.

In a *a*-Si:H:P, the quasi-Fermi level F_n lies above E_F . The transitions from states between F_n and E_F into the CB produce PA. Its onset is approximately at $E_c - F_n$; we used it for determining $E_c - F_n$. F_n depends on the pump intensity and temperature. The dependence of $E_c - F_n$ on the pump intensity is logarithmic in carrier density, which is a sublinear function of the pump intensity; it is not surprising that we could hardly detect it when we changed the pump intensity by about one order (which was the experimentally feasible range). However, the dependence of $E_c - F_n$ on temperature was clearly observed [see Fig. 3(a)]; it has the expected trend.

In the dark, there are transitions from the VB into the states between F_n and E_F , which are eliminated by illumination; they produce PB at the high-energy end of the PM spectrum. Its onset is at $E_F - E_v$, but the DOS at E_F is low and the determination of $E_F - E_v$ is inaccurate. Therefore, we obtained E_F from measuring the activation

energy $E_\sigma = E_c - E_F$ of electrical conductivity. Analogous considerations apply to *a*-Si:H:B. The Fermi and quasi-Fermi energies are listed in Table I.

In the fitting procedure, we assume that the matrix elements of the various contributions to $\Delta\alpha$ are constant (within the band of each contribution). Then, $\Delta\alpha$ for each contribution is proportional to the energy-conserving convolution of the changes in the densities of initial and final states. The procedure is described in Ref. 24.

The adjustable parameters used for fitting the spectra are

$$a\text{-Si:H: } E(D_i^0), E(D_i^-), \Delta E_D,$$

$$a\text{-Si:H:P: } E(D_P^0), E(D_P^-), \Delta E_D, E_0^c, E_c - F_n,$$

$$a\text{-Si:H:B: } E(D_B^0), \Delta E_D, E_0^v, F_p - E_v.$$

The values for optimum fits are given in Tables I and II. In addition to the above parameters, the various contributions to the $\Delta\alpha$ spectrum have different strengths associated with different matrix elements and different absolute values of the densities [constants A and B in Eqs. (1) and (2)]. From fitting the spectra, we can only determine the relative strengths, for example the strength of $D^- \rightarrow \text{CB}$ (PA) vs $\text{VB} \rightarrow D^-$ (PB). These relative strengths are given in Table I. As seen in Fig. 5, the fits obtained with this procedure are very good.

The result of this analysis is the determination of the distribution of states in the gap shown in Figs. 2(a)–2(c).

TABLE I. Properties of P- and B-doped samples ($T=80$ K). In the first column, the doping levels (PH_3/SiH_4 or $\text{B}_2\text{H}_6/\text{SiH}_4$) in the gas are listed. Energies are in eV. $G(P_4)/G(D_P)$ is the ratio of the density of P_4 states relative that of D_P states, obtained from the ratio of the spectral strengths assuming that the matrix elements of transitions involving P_4 states and D_P states are the same. This is certainly not the case. However, it seems plausible to assume that these matrix elements do not change with Q and LS. In this case, the observed changes in $G(P_4)/G(D_P)$ produced by Q and LS [with respect to $G(P_4)/G(D_P)$ in the A sample] are the changes in the density ratio $G(P_4)/G(D_P)$ produced by these treatments. Analogous considerations apply to the boron doped sample. The $\Delta G(D_i)/G(D_P)$ column gives the ratio of the spectral strength of the D_i states in *a*-Si:H:P generated by LS to the spectral strength of the D_P states in the LS sample. We refer to Sec. V for a discussion of D_i defects in *a*-Si:H:P.

Sample	Status	$E_c - E_F$	$E_c - F_n$	$E_F - E_v$	$F_p - E_v$	E_0	$G(P_4)/G(D_P)$	$\Delta G(D_i)/G(D_P)$	$G(B_4)/G(D_B)$
<i>a</i> -Si:H:P 0.01 at. %	A	0.24	0.17			0.06	24	0	
	Q	0.24	0.16			0.06	27	0	
	LS(1 h)	0.62	0.19			0.06	23	61	
0.1 at. %	A	0.24	0.15			0.07	11	0	
	Q	0.24	0.15			0.07	12	0	
	LS(1 h)	0.60	0.16			0.07	6.9	23	
	LS(2 h)	0.61	0.16			0.07	4.8	54	
	LS(4 h)	0.62	0.17			0.07	4.8	109	
1.0 at. %	A	0.28	0.14			0.08	3.7	0	
	Q	0.27	0.15			0.08	3.7	0	
	LS(1 h)	0.45	0.18			0.08	3.9	0	
<i>a</i> -Si:H:B 0.1 at. %	A			0.33	0.21	0.11			4.4
	Q			0.34	0.22	0.11			4.5
	LS(2.5 h)			0.36	0.23	0.11			4.1

TABLE II. Defect energies. Energies (in eV) of the D states measured from the bottom of the conduction band E_c . Energy gap $E_g = 1.78$ eV for undoped samples, 1.82 eV for doped samples.

Sample	$E(D_i^0)$	$E(D_i^-)$	$E(D_p^0)$	$E(D_p^-)$	$E(D_B^0)$	ΔE_D
a -Si:H	1.10	0.60				0.21
a -Si:H:P			1.21	0.95		0.23
a -Si:H:B					0.54	0.18

The energies and the widths of the DOS distributions are the actual values; the relative strengths are arbitrary.

The dependence of the PM spectra of a -Si:H:P on temperature and doping level is shown in Fig. 3. The temperature dependence of the shape of the spectrum of the heavily doped sample (1 at. % $[\text{PH}_3]/[\text{SiH}_4]$) is small, but the onset changes are significant [inset in Fig. 3(a)]; the origin of the observed shift is discussed above. Doping produces some changes in the shape of the PM spectrum when it is heavy [Fig. 3(b)] (a deeper drop in the middle which corresponds to stronger PB produced by a relatively larger density of dangling bonds).

In Fig. 4, we plot the dependence of the ratio of the

density of P_4 states to that of D_p states as a function of the doping level; this plot was obtained from Table I, assuming that the matrix elements do not change with doping. Figure 4 shows that this ratio which is related to the "doping efficiency" decreases with the doping level.

IV. CHANGES IN THE PM SPECTRA PRODUCED BY LS AND Q

LS and Q produce changes in the PM spectra as seen in Fig. 5, both in the strength and shape. The changes in the strength of various transitions cannot be associated directly with the changes of the densities of corresponding states in the gap, even if we assume that the matrix elements do not change with these treatments. The reason is that we are dealing with steady-state photoinduced spectra, which are proportional to the steady-state photocarrier densities. Therefore their strength (measured with the same pump intensity) depends on the recombination process, which is related to the changes in the state density in a complex and unknown way. Consequently, changes in the spectral shape are much easier to interpret. Assuming that the matrix elements are the same as in the annealed sample, we can obtain from the PM spectra the *relative* change in the densities in the gap produced by LS and Q, provided we take into proper account the shifts of the Fermi and quasi-Fermi levels.

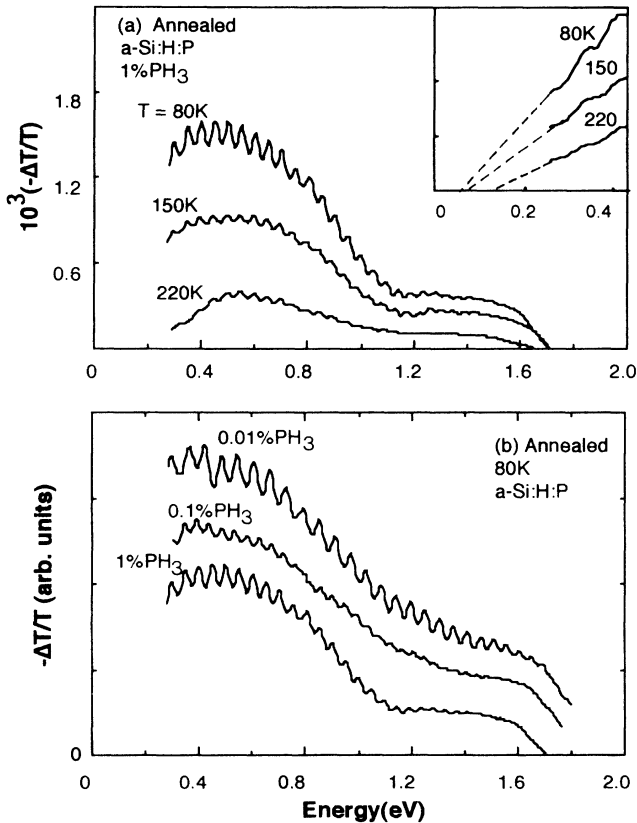


FIG. 3. (a) PM spectra of annealed a -Si:H:P ($[\text{PH}_3]/[\text{SiH}_4] = 1$ at. %) measured at different temperatures for the same pump intensity. The inset shows the temperature dependence of the onset. (b) PM spectra of a -Si:H:P measured at 80 K for different doping levels.

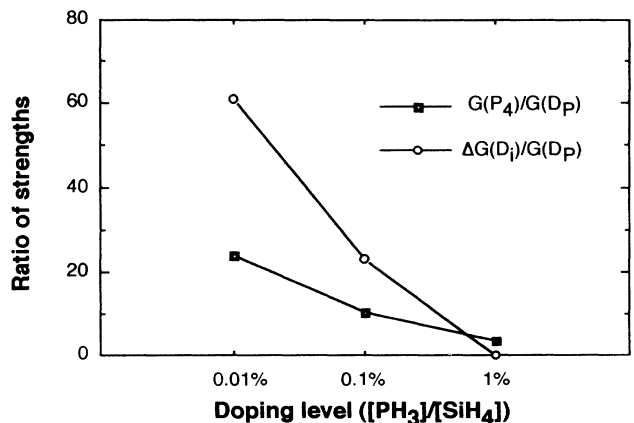


FIG. 4. Dependence of the ratio of the P_4 density vs D_p density in the dark on the doping level. The ratio is in arbitrary units, however its dependence on doping is correct if we assume that the matrix elements do not change with doping. The same consideration applies also to the doping-level dependence of the density of D_i vs D_p in LS samples (the LS exposure time was 1 h).

In this section, we will present and analyze the LS and Q results obtained for *a*-Si:H, *a*-Si:H:P, and *a*-Si:H:B.

A. Undoped *a*-Si:H

As seen in Fig. 5(a), LS produces a small shift of the PM band and an increase in its strength. Assuming that the matrix elements do not change, the strength change is due to the combined effect of the defect density increase (increasing the strength) and the change of the recombination time (decreasing with the increased defect density). Apparently, in this case, the defect density increase prevails over the recombination time decrease in determining the strength of the PM band. Both the increased density of the *D* states and shorter recombination time

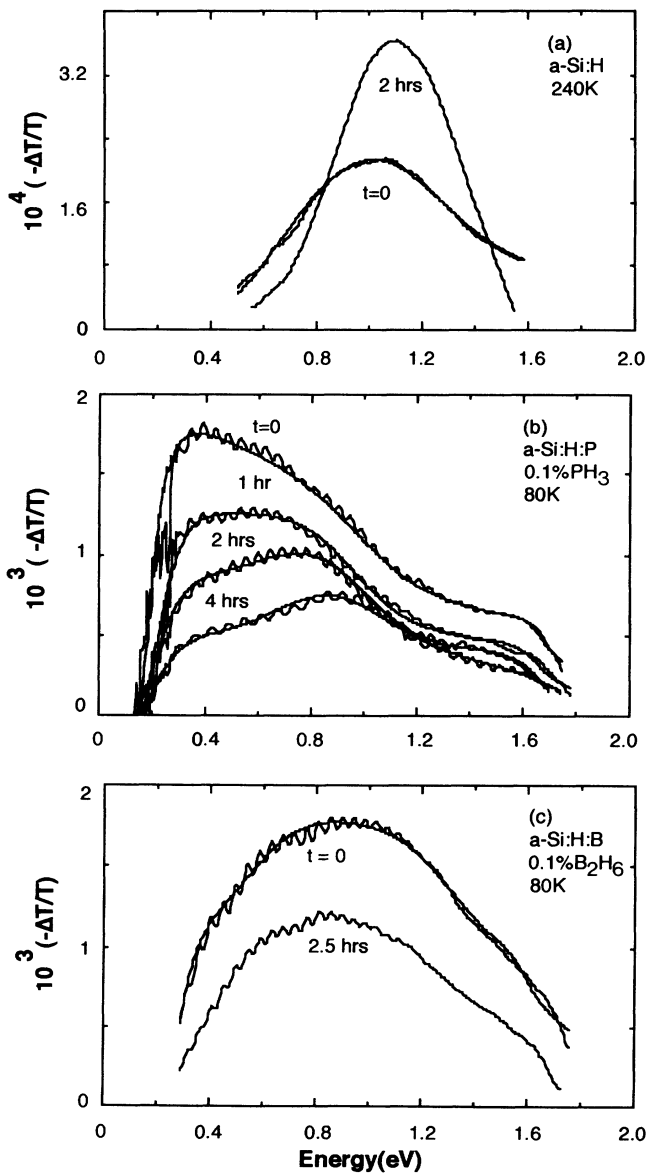


FIG. 5. Comparison of the PM spectra of annealed ($t=0$) and LS samples. The solid curves passing through the measured curves are fits explained in the text.

push the quasi-Fermi levels F_n and F_p away from the band edges. This shift leads to the narrowing of the PM band width, in agreement with the data [Fig. 5(a)].

B. Phosphorus-doped *a*-Si:H

As seen in Fig. 5(b), LS produces strong changes in the PM spectrum of *a*-Si:H:P.²⁵ As the LS exposure increases, more and more of the oscillator strength is shifted from the low-energy end to the middle of the spectrum. To analyze the spectrum of LS *a*-Si:H:P, we tried the same procedure described in the preceding section for annealed *a*-Si:H:P (using tail states and D_p defects). However, we were not able to obtain a reasonable fit. Obviously, the spectra of LS samples indicate [Fig. 5(b)] that some additional strength has to be added in the middle range, that is in the region of the PM bands in undoped *a*-Si:H that are associated with the D_i defects. After adding D_i effects with Gaussian distributions, using the peak energies and widths given in Table II in the fitting procedure, we have obtained an excellent fit to the measured spectra of the LS samples. The relative strength of these

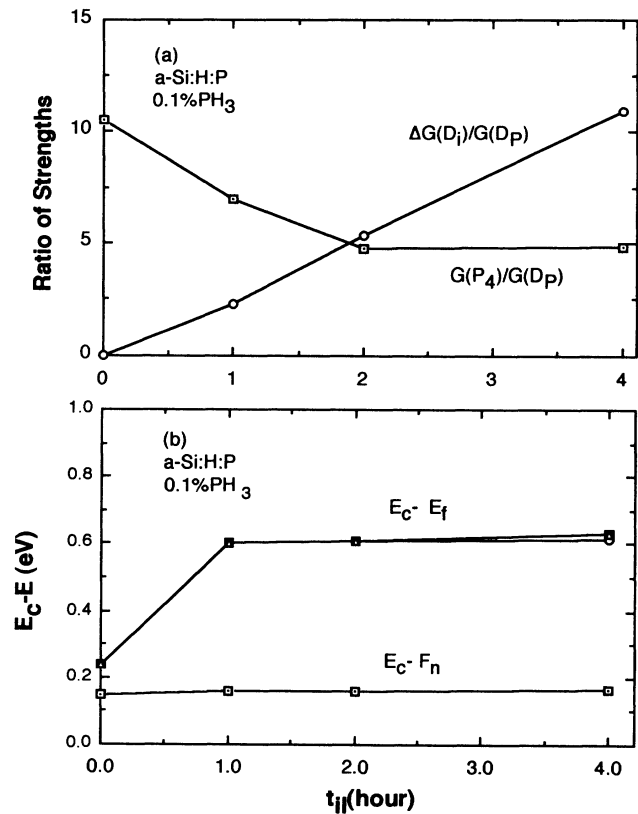


FIG. 6. (a) P_4 and D_i densities vs D_p density as a function of LS exposure time t_{ij} . Similar comments apply as for Fig. 4. (b) Positions of the Fermi level and quasi-Fermi level (for constant illumination) as a function of LS exposure time. The curve determined from the temperature dependence of electrical conductivity is not distinguishable from the curves calculated from the data in (a), using Eq. (6) whether we assume that $\Delta G(D_i)$ is constant or increases as $t_{ij}^{1/3}$.

D_i defects vs D_p defects was an adjustable parameter and is given in Table I in the $\Delta G(D_i)/G(D_p)$ column. The D_i defects in a -Si:H:P are discussed in more detail in Sec. V. Another adjustable parameter was the relative strength of the P_4 (band-tail) states vs the strength of D_p [column $G(P_4)/G(D_p)$ in Table I]. In this table, we also give the positions of the Fermi-level E_F (determined from conductivity measurements) and quasi-Fermi level F_n (determined from the onset of the PM spectra) for the doping levels $[\text{PH}_3]/[\text{SiH}_4]=0.01$ at. %, 0.1 at. %, and 1 at. %.

The distribution of the gap states in LS a -Si:H:P is shown in Fig. 2(d). In Fig. 6(a), we show (for the doping level of 0.1 at. %) the ratio of $G(P_4)/G(D_p)$ as a function of the LS exposure time. We note that LS first increases the density of D_p defects relative to the P_4 states, but the process eventually saturates. In this figure, we also plot the density $\Delta G(D_i)$ of the intrinsic defect D_i generated by LS relative to the density of D_p . We note that it linearly increases with the LS exposure. In Fig. 6(b), we show the changes of E_F and F_n with the exposure time. The Fermi level goes deeper into the gap with LS exposure, but reaches a saturation. The position of the quasi-Fermi level (measured at the same pump intensity) changes only slightly because it is in a region of high BT state density [Figs. 2(b), 2(d)].

In Fig. 7, the PM spectra of a -Si:H:P, after 1- and 2- h LS exposure times for the doping levels of 1 at. % and

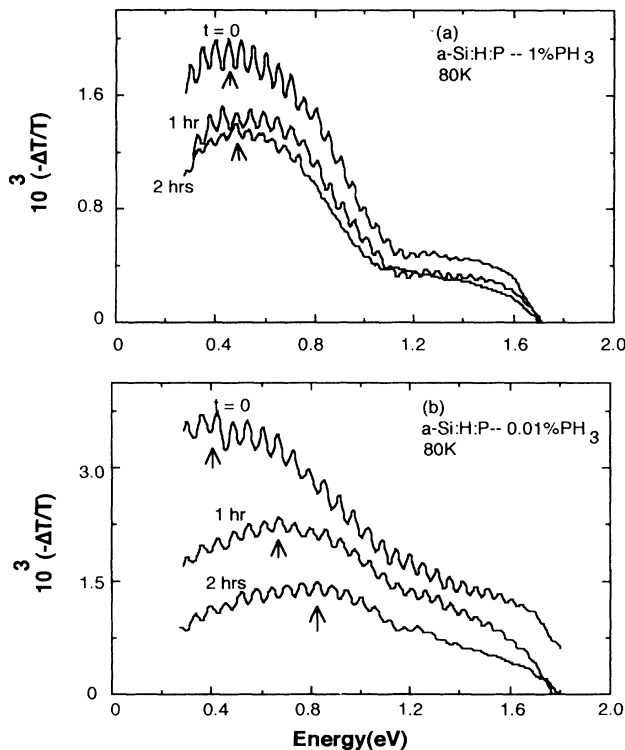


FIG. 7. PM spectra of a -Si:H:P with different doping levels (1 at. % and 0.01 at. %) in the annealed state ($t=0$) and after LS exposure of 1 and 2 h (constant pump intensity level).

0.01 at. % are shown. We note that the changes produced by LS are much stronger in the less doped sample. The generation of “intrinsic” defects D_i decreases with increasing doping level, as seen in Fig. 4. The ratio of $\Delta G(D_i)/G(D_p)$, determined for the same exposure time (1 h) decreased to almost zero when the doping level changed from 0.01 at. % to 1 at. %.

The thermal quenching (Q) data are shown in Fig. 8 for various doping levels (data on A and LS samples are also plotted for comparison). The PM spectra of the most lightly and most heavily doped samples are hardly different in the A and Q states; in the sample doped at 0.1 at. %, the quenching significantly increased the strength, but the spectral shape is similar as in the annealed sam-

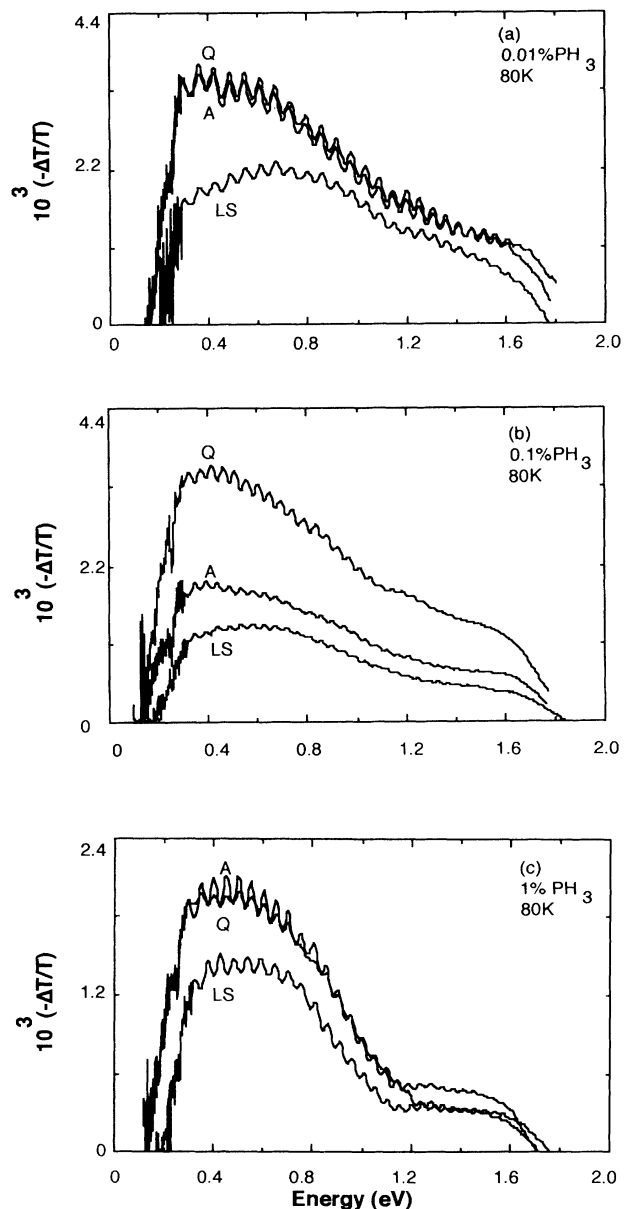


FIG. 8. PM spectra of annealed, quenched and LS (exposure time of 1 h) samples of a -Si:H:P with different doping levels.

ple. The fitting revealed some changes produced by the thermal quenching process; the fitting parameters are listed in Table I. Generally, one observes an increase in the ratio of $G(D_4)/G(D_P)$ states, which is larger when the doping level is smaller.

C. Boron-doped *a*-Si:H

The PM spectra of *a*-Si:H:B are little changed by LS, as seen in Fig. 5(c). Also, Q does not change the PM spectrum (Fig. 9). We may speculate that the density of defects is very high in the dark and is relatively little effected by LS or Q (in the same sense that heavily doped *a*-Si:H:P is rather insensitive to these treatments).

We have observed a remarkable effect in "as-deposited" samples before they were exposed to LS or Q. The spectrum of this "virgin" sample (V) is shown in Fig. 9. At the high-energy end, we note photoinduced bleaching (ΔT is positive in this region). We consider this observation as a support for our interpretation of the spectra.²⁶ In our model, it is the $B_4^- \rightarrow CB$ transition [Fig. 1(c)] which is bleached by the pump. In most materials, these bleaching transitions involving defect D and the more distant band are not strong enough to prevail over the PA transitions and produce only a decrease of $-\Delta T$ without crossing the zero. At still higher energies, we observe increased absorption (PA) produced by the thermal shift of the absorption edge E_g . Therefore, normally $-\Delta T$ does not cross the zero, but apparently virgin *a*-Si:H:B is an exception. The PM spectra of an annealed, quenched, or LS sample no longer shows this bleaching region (Fig. 9). The fitting parameters for the A, Q, and LS samples are listed in Table I.

V. D_i DEFECTS IN LS *a*-Si:H:P

The conclusion that in LS *a*-Si:H:P there are D_i^0 states in the dark below the Fermi level E_F may be confusing. However, the existence of such states follows from the presence of a positive correlation energy. Adler and

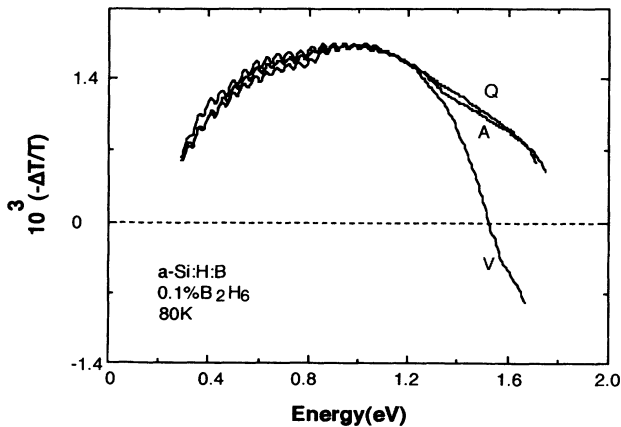


FIG. 9. PM spectra of virgin (as-deposited) (V), annealed (A), and quenched (Q) *a*-Si:H:B.

Yoffa²³ show that the full conversion of D_i^0 into D_i^- occurs when the Fermi level E_F is above the D_i^- distribution; as long as E_F is inside the D_i^- distribution, there are some D_i^0 states in thermal equilibrium state. In LS *a*-Si:H:P, E_F is indeed deep inside the D_i^- distribution, as seen in Fig. 2(d).

In Fig. 2(b), we see that in annealed *a*-Si:H:P, E_F is above the D_i^- distribution [this distribution is shown in Figs. 2(a) and 2(d)]. Therefore, in A *a*-Si:H:P, the D_i defects are in the D_i^- state in the dark; their distribution overlaps with that of D_P^- and the D_i^- 's only broaden the distribution of D_P^- . Consequently, it may not be possible to distinguish between D_P^- and D_i^- defects. These D_i defects can become observable only when the Fermi level is moved toward midgap.

We will now discuss how the density $\Delta G(D_i)$ of the D_i states in LS *a*-Si:H:P, as shown in Table I and Fig. 6(a), is defined, and how it was determined from the PM spectra. We shall first discuss how the spectrum depends on the position of the Fermi level E_F .

Let us start with E_F inside the D_i^0 band, and assume that the temperature is zero. The density of electrons in D_i^0 states is

$$n(D_i^0) = G(D_i) \int_{-\infty}^{E_F} g_0(E) dE, \quad (4)$$

where $G(D_i)$ is the total density of D_i defects and $g_0(E)$ is a normalized Gaussian distribution [$\int_{-\infty}^{+\infty} g_0(E) dE = 1$] centered at $E(D_i^0)$. There are no electrons in D_i^- states. When E_F is in the gap between the D_i^0 and D_i^- distributions, then $n(D_i^0) = G(D_i)$. This is the situation described in Sec. III for undoped *a*-Si:H.

When E_F enters into the D_i^- band, the electron densities are given by the equations

$$n(D_i^-) = 2G(D_i) \int_{-\infty}^{E_F} g(E) dE, \quad (5a)$$

$$n(D_i^0) = G(D_i) - \frac{1}{2}n(D_i^-). \quad (5b)$$

Function $g(E)$ is the same Gaussian as $g_0(E)$ in Eq. (4), but centered at $E(D_i^-)$.

It follows from the discussion in Sec. III that electrons in D_i^0 and D_i^- states produce contributions to the PM spectra with opposite signs. We see in Fig. 1 that if the sample in the dark has D_i^0 states, upon illuminations transitions $D_i^0 \rightarrow CB$ are bleached (PB) and transitions $D_i^- \rightarrow CB$ are generated (PA). But if the sample in the dark has D_i^- states, transitions $D_i^- \rightarrow CB$ are bleached and transitions $D_i^0 \rightarrow CB$ are generated. Therefore, when we have both D_i^0 and D_i^- states in the dark, it follows from Eqs. (5) that the PM signal is proportional to

$$\Delta G(D_i) = n(D_i^0) - \frac{1}{2}n(D_i^-) = G(D_i) \left[1 - 2 \int_{-\infty}^{E_F} g(E) dE \right]. \quad (6)$$

The factor $\frac{1}{2}$ in the above equation is due to the fact that only one electron of the doubly occupied D_i^- states can make the transition $D_i^- \rightarrow CB$.

Equation (6) is only an approximation for describing the PM spectrum of D_i . The above-mentioned rule that

the contribution of the D_i^0 and D_i^- states has opposite sign leads to exact cancellations only for sharp energy levels. For distributions, changes in the position of E_F produce changes not only in the total electron density but also in the shape of the occupied D_i^- band. For example, if E_F is in the middle of the D_i^- band, Eq. (6) gives zero PM signal ($\Delta G=0$), which is exactly true for sharp energy levels. For distributions, it is only an approximation. Another approximation is taking the electron occupation ($T=0$ K situation) instead of the exact occupation function at $T=80$ K (which in this case is different from the simple Fermi distribution function²³). We checked that a simple kT smearing at 80 K of the step function does not produce a detectable difference in the fitting.

From the fitting of the data, we have determined $\Delta G(D_i)/G(D_P)$, which is shown in Table I and Fig. 6(a). We see that $\Delta G(D_i)/G(D_P)$ increases linearly with LS exposure time t_{il} . If we want to obtain information about the generation of D_i states by LS, we first have to know the dependence of $G(D_P)$ on t_{il} . According to Stutzmann, Biegelsen, and Tsai,^{15,16} $G(D_P) \sim t_{il}^{1/3}$. Since $\Delta G(D_i)/G(D_P) \sim t_{il}$ [Fig. 6(a)], $\Delta G(D_i) \sim t_{il}^{4/3}$. This LS time dependence can be produced by the LS time dependence of both $G(D_i)$ and the integral in Eq. (6) (that is, by the dependence of E_F on t_{il}). Let us consider two cases: (i) $G(D_i)$ increases with LS in the same way as $G(D_P)$ ($\sim t_{il}^{1/3}$); (ii) $G(D_i)$ does not depend on LS [it is the same as in the annealed sample and the observed dependence of $\Delta G(D_i)$ on t_{il} is due to the shift of the Fermi level]. In the first case, the parenthesis in Eq. (6) is proportional to t_{il} ; in the second case, it is proportional to $t_{il}^{4/3}$. We calculate the dependence of E_F on t_{il} for both cases from Eq. (6), using the measured position of E_F in the annealed sample ($t_{il}=0$). The result is shown in Fig. 6(b), and compared with E_F in LS samples measured from the temperature dependence of electrical conductivity. We see that the fit is good for both assumptions (i) and (ii), and we cannot distinguish between them on the basis of our data. The basic agreement between E_F calculated from the spectra and E_F determined from electrical conductivity gives a strong support to the model, although in view of the approximations made in the calculations and fittings the high accuracy of agreement is likely to be accidental.

VI. DISCUSSION AND CONCLUSIONS

The energy levels and the origin of deep defects in *a*-Si:H has been a long lasting matter of controversy.^{10,27} The basic problem has been the different D^- energies in undoped and P-doped *a*-Si:H, which has led to the model of intimate pairs,⁹ and later to a more general defect pool model.¹¹ The attempt to use light phosphorus doping to observe the transition from isolated D_i^- to the paired D_P^- state has failed²⁸ because the D_i^- state in undoped *a*-Si:H is unoccupied and D_i^0 overlaps with D_P^- . The recent field effect experiments²⁹ lend support to the defect pool model; however, there is an uncertainty related to the fact that the field effect is strongly sensitive to the surface states.

The basic idea of both the intimate pair and defect pool

models is that there are at least two different defects in *a*-Si:H. From this point of view, it is very important that by the PM spectroscopy, which is clearly bulk controlled, we observe two defects (D_i^- and D_P^-) on one sample (lightly P-doped *a*-Si:H), the state of which is controlled by the light soaking.

There is a question about how much credibility one can give to the results obtained by spectra fitting. We note that the main features are already observed in the raw spectra. For example, any analysis of the PM spectra of LS *a*-Si:H:P has to include some states in the middle of the spectral range to explain the features seen in Fig. 5(b). This is the origin of our main argument about the D_i defects generated (or revealed) by LS, which we cast into a more quantitative form by making assumptions about the gap-state distributions.

Banerjee *et al.*³⁰ observed in *a*-Si:H:P a state in the same energy range as our D_i^- state, using isothermal capacitance transient spectroscopy (ICTS). They call this an "isolated" dangling bond. This defect was seen in the rested sample, but its strength increased with LS. It was negatively charged in the dark. It may be the same defect as our D_i . If E_F is inside the distribution of D_i^- , both D_i^0 and D_i^- states should be present, and the method used in Ref. 30 detected the D_i^- states.

A study of the light soaking of the similarly P-doped *a*-Si:H has been recently performed by Stitzl, Kotz, and Muller.³¹ They studied the changes of the electrical conductivity and the density of the deep defects, the total concentration of which was determined by photodeflection spectroscopy (PDS). The observed conductivity changes produced by light soaking (or radiation damage) were compared with two models. In the first one a deep defect (D) with an energy $E_c - E = 0.5$ eV and a constant number of the active donors was considered. In the second one the energy of the deep defect (D), $E_c - E = 0.9$ eV, was assumed, and the number of the active donors was adjustable. Stitzl, Krotz, and Muller³¹ preferred the second possibility, and found that the adjusted number of the active donors is equal to the number of deep defects (dangling bonds), which is in agreement with the autocompensation theory of doping.³¹

Our photomodulation results enabled us to find the energy levels of the light-induced defects. The fact that at least part of the light-induced defects in lightly P-doped *a*-Si:H must have energies around $E_c - E \approx 0.6$ eV seems to support the first possibility discussed by Stitzl, Krotz, and Muller.³¹ Can we somehow explain these seemingly controversial results?

Recently, Leen and Cohen³² observed in lightly P-doped *a*-Si:H two energy levels: One at $E_c - E \approx 0.6$ eV and the second at $E_c - E \approx 0.9$ eV. They argue that these states are two modifications of the same center. They attribute the shallow state at $E_c - E \approx 0.6$ eV, observed shortly after $D^0 \rightarrow D^-$ conversion, to the "unrelaxed" D^- state, and label it as $(D^-)^*$, while the deeper state at $E_c - E \approx 0.9$ eV is the stable "relaxed" D^- state.³³

The following idea may reconcile our results with those of Stitzl, Krotz, and Muller. dc conductivity and PDS are steady-state measurements, and therefore controlled

by the relaxed (0.9-eV) state. During the photomodulation measurements, there is a continuous interconversion of D^0 and D^- states, and if the unrelaxed $(D_i^-)^*$ state³² has a sufficiently long lifetime, a certain fraction of all D^- states are in the $(D^-)^*$ state. This state, labeled in our notation as D_i^- , may be detected by PM spectroscopy but not by dc conductivity.

The PM spectroscopy is one of the few methods which can detect such an unrelaxed state, the "observation window" of which is very narrow.³² Naively, one would expect that with increasing doping the number of the "unrelaxed" states $(D_i^-)^*$ should increase. The observation that the $\Delta G(D_i^-)/G(D_p)$ ratio decreases with increasing doping (Fig. 4) can be explained by the shift of the Fermi level with doping and by Fermi-level-dependent relaxation lifetime, which decreases with increasing doping. Although in principle the model of Leen and Cohen³² may be able to explain our results, as well as the results of Stitzl, Krotz, and Muller,³¹ and the DLTS (deep level transient spectroscopy) versus ICTS controversy,³⁴ more studies are necessary for a clear proof of the correctness of the defect pool or intimate pair models used for the explanation of the shift of the D^- (D^+) position in doped a -Si:H.

As concerns the concentration of active donors, both Stutzmann³ and Stitzl, Krotz, and Muller³¹ came to the conclusion that LS (or radiation damage³¹) increases the concentration of active donors, approximately in proportion to the number of deep defects.³¹ On the other hand, the quasi-independent changes of the density of active donors and deep defects have been claimed by other groups.^{32,34} We cannot clarify this problem, due to the fact that we have labeled by P_4 the sum of the active donors and conduction-band tail states, because we cannot distinguish them by PM spectroscopy. As has been shown by Stutzmann,³ LS leads to anticorrelated change of occupied donor and tail states so that their sum (our

P_4) is approximately constant. The slight decrease of the $G(P_4)/G(D_p)$ density ratio observed in the PM spectrum indicates small LS-induced increase of D_p states.

We can summarize the main conclusions from this study as follows.

(1) LS strongly changes the shape of the PM spectrum of phosphorus-doped a -Si:H, while the changes in undoped and boron-doped samples are small. In undoped a -Si:H, LS increases the density of dangling bonds ("intrinsic" D_i defects); the quasi-Fermi levels move closer to the middle of the gap, and this produces PM band sharpening.

(2) To fit the PM spectra of LS a -Si:H:P, we need to introduce, in addition to D_p states, D_i^0 and D_i^- states with similar properties as these states have in undoped a -Si:H. These states can be observed because LS shifts the Fermi level toward midgap. We cannot determine from the data whether the D_i defects exist in the annealed state and are made visible by LS, or whether they are actually generated by LS. The existence of D_i^0 states in the dark in LS a -Si:H:P is possible because of the positive electron correlation energy of this defect.

(3) Thermal quenching usually produces small changes in the PM spectra. The changes observed in a -Si:H:P can be interpreted as due to the increase of the density of P_4 states relative to D_p defects.

ACKNOWLEDGMENTS

We are grateful to Joseph Shinar for providing us with boron-doped a -Si:H samples, in which we first saw photoinduced transmission. We thank Z. Vardeny for valuable discussions and T. R. Kirst for technical assistance. This work was partly supported by National Science Foundation Grant No. DMR-9014977 (Brown University) and the Czechoslovak Academy of Sciences Grant No. 11063 (Institute of Physics).

¹D. L. Staebler and C. R. Wronski, *J. Appl. Phys.* **51**, 3262 (1980).

²M. Stutzmann, *Philos. Mag. B* **56**, 63 (1987).

³M. Stutzmann, *Phys. Rev. B* **35**, 9735 (1987).

⁴W. B. Jackson, M. Stutzmann, and C. C. Tsai, *Sol. Cells* **21**, 431 (1987).

⁵W. B. Jackson, *Phys. Rev. B* **41**, 10257 (1990).

⁶T. M. Leen, J. D. Cohen, and A. V. Gelatos, in *Amorphous Si Technology*, edited by P. C. Taylor *et al.*, MRS Symposia Proceedings No. 192 (Materials Research Society, Pittsburgh, 1990), p. 707.

⁷R. A. Street, J. Kakalios, C. C. Tsai, and T. M. Hayes, *Phys. Rev. B* **34**, 3030 (1986); J. Kakalios and T. M. Hayes, *ibid.* **34**, 6014 (1986).

⁸R. A. Street, J. Zasz, and M. J. Thomson, *Appl. Phys. Lett.* **43**, 672 (1983).

⁹J. Kočka, *J. Cryst. Solids* **90**, 91 (1987).

¹⁰J. Kočka, M. Vaněček, and A. Trřiska, in *Amorphous Silicon and Related Materials*, edited by H. Fritzsche (World Scientific, Singapore, 1988).

¹¹Z. E. Smith and S. Wagner, in *Amorphous Silicon and Related Materials* (Ref. 10), p. 409.

¹²Z. Vardeny and J. Tauc, *Phys. Rev. Lett.* **54**, 1844 (1985); Y. Bar-Yam, J. D. Joannopoulos, and D. Adler, *ibid.* **55**, 138 (1985).

¹³T. X. Zhou, Ph.D. thesis, Brown University, 1989.

¹⁴H. T. Grahn, C. Thomsen, and J. Tauc, *Opt. Commun.* **58**, 226 (1986).

¹⁵M. Stutzmann, D. K. Biegelsen, and C. C. Tsai, *Phys. Rev. B* **32**, 23 (1985).

¹⁶M. Stutzmann, *Appl. Phys. Lett.* **56**, 2313 (1990).

¹⁷Z. Vardeny, T. X. Zhou, H. A. Stoddart, and J. Tauc, *Solid State Commun.* **65**, 1049 (1988).

¹⁸In our discussion of the dangling-bond states, we neglect the lattice relaxation of the charged states (Ref. 12). In our symmetrical model, the lattice relaxation energy $\Delta E_r = E(\text{PA}) + E(\text{PB}) - E_g$ is small in a -Si:H. From Table II, one has for the D_i defect in a -Si:H, $E(\text{PA}) + E(\text{PB}) = 1.7$ eV, which is within 0.1 eV equal to the gap energy. For this material, the neglect of ΔE_r is justified; we assumed that the lattice relaxation is negligible in the doped samples as well.

¹⁹In undoped a -Si:H, transitions involving the band-tail states (which in this case are due to distorted bonds) are observed at low temperatures (Ref. 24).

- ²⁰Photogenerated D_p^0 produces another PA transition $VB \rightarrow D_p^-$. The energy of this transition (0.9 eV) is close to the energy of the PB transition $D_p^- \rightarrow CB$ (0.95 eV) and these contributions to the PM spectrum overlap. What we measure is the net effect of this superposition which is PB (an experimental fact). The actual strength of the PB transition $D_p^- \rightarrow CB$ is larger than we calculated from the spectra. The same approximation was made in Ref. 17.
- ²¹In Ref. 17, a Gaussian function was used for the tail states in a -Si:H:P. We have obtained a good fit to our data using an exponential instead of a Gaussian. The reasons that the fitting is not very sensitive to the exact form of the BT distribution function is that the PM signal is determined by the density of states between F_n and E_F , which usually is a small part of the distribution function [see Figs. 2(b) and 2(c)].
- ²²J. G. Simmons and G. W. Taylor, *Phys. Rev. B* **4**, 502 (1971).
- ²³D. Adler and E. J. Yoffa, *Phys. Rev. Lett.* **36**, 1197 (1976).
- ²⁴H. A. Stoddart, Z. Vardeny, and J. Tauc, *Phys. Rev. B* **38**, 1362 (1988).
- ²⁵The structures seen on the onsets of the PM spectra in Fig. 5(b) are due to the changes of the Si—H bond vibrations produced by changing the sample temperature. We identified this thermal effect by measuring the infrared (dark) spectra at two different temperatures; we found that the differences between the spectra have the same structure as the structures seen on the onsets of the PM spectra. The photoinduced vibrational spectra in a -Si:H were first observed by Z. Vardeny and M. Olsakier [*J. Non-Cryst. Solids* **97/98**, 109 (1987)].
- ²⁶We first observed the $-\Delta T < 0$ region in the spectrum of virgin a -Si:H:B in the samples made by J. Shinar's group at Iowa State University. Because this feature easily disappeared we considered it accidental. However, we observed it again in the samples prepared in Prague, and are now confident that it is a real property of (at least some) virgin samples.
- ²⁷D. V. Lang, J. D. Cohen, I. P. Harbison, M. C. Chen, and A. M. Sergent, *J. Non-Cryst. Solids*, **66**, 217 (1984).
- ²⁸J. D. Cohen and A. V. Gelatos, in *Proceedings of the 19th International Conference on the Physics of Semiconductors*, edited by W. Zawadski (Polish Academy of Science, Warsaw, 1988), p. 1629.
- ²⁹J. D. Powell, C. van Berkel, and S. C. Deane, *J. Non-Cryst. Solids* **137/138**, 1215 (1991).
- ³⁰R. Banerjee, T. Furui, H. Okushi, and K. Tanaka, *Appl. Phys. Lett.* **53**, 1829 (1988).
- ³¹H. Stitzl, G. Krotz, and G. Muller, *Appl. Phys. A* **52**, 335 (1991).
- ³²T. M. Leen and J. D. Cohen, *J. Non-Cryst. Solids* **137/138**, 319 (1991).
- ³³Note that this relaxation of light-induced defects proposed by Leen and Cohen (Ref. 32) is different from the relaxation of "natural" defects (present in annealed samples).
- ³⁴H. Okushi, N. Orita, K. Arai, and K. Tanaka, *J. Non-Cryst. Solids* **137/138**, 175 (1991).